# Breakdown of structural models for vibrations of single-wall zigzag carbon nanotubes

S. S. Gupta, F. G. Bosco, and R. C. Batra[a)]
*Department of Engineering Science and Mechanics, Virginia Polytechnic Institute and State University, M/C 0219, Blacksburg, Virginia 24061, USA*

(Received 12 April 2009; accepted 22 August 2009; published online 24 September 2009)

Free vibrations of zigzag single-wall carbon nanotubes (SWCNTs) of aspect ratio (length/diameter) ~6 and with ends traction-free have been studied using molecular mechanics (MM) simulations with the MM3 potential. It is found that the frequencies of inextensional (the Love and the Rayleigh) modes of an $(n, 0)$ SWCNT saturate at the circumferential wave number of either $(n-1)/2$ or $n/2$ where $n$ is odd or even. This is explained in terms of its molecular structure. Since the frequencies of the inextensional modes of vibration of a thin cylinder made of an isotropic linear elastic material do not saturate with an increase in the circumferential wave number, a continuum structure *cannot* represent all modes of vibration of a zigzag SWCNT. This result is independent of the value assigned to the wall thickness of the SWCNT. We have also found values of material and geometric parameters of a shell and a hollow cylinder by equating their frequencies of the inextensional, the radial breathing, the axial and the torsional modes of vibrations to the corresponding ones of a zigzag SWCNT, and by taking their mean diameter and length equal to those of the SWCNT. The frequencies of the extensional modes of oscillations of the two continuum structures for various axial half wave numbers and circumferential wave numbers are found to match well with those of the SWCNT obtained from the MM simulations. However, the frequencies of the inextensional modes of the continuum structures deviate noticeably from those of the SWCNT, and this deviation increases with an increase in the circumferential wave number. © *2009 American Institute of Physics*. [doi:10.1063/1.3232206]

## I. INTRODUCTION

Since their discovery by Iijima,[1] static deformations and vibrations of single- and multi-wall carbon nanotubes (SWCNTs/MWCNTs) have been studied experimentally, numerically through molecular mechanics/dynamics (MM/MD) simulations, and by using quantum mechanics, structural mechanics, and continuum mechanics theories. Methods based on structural theories give results whose accuracy depends on assumptions made to derive a structural model of a carbon nanotube (CNT). For example, using a beam, a shell, a hollow cylinder, or a solid fiber to study the deformations of a SWCNT requires different levels of effort, and yields quite distinct results that may not be close to those found through MM/MD simulations. Furthermore, in structural models, one may simulate a bond between adjoining atoms as a beam, a spring, or a truss. The inherent difficulty is to determine the mechanical properties of the material of the beam, the spring, and the truss from those of the relevant MM/MD potential. Alternatively, one can use the Cauchy–Born rule (or its modification) and the interatomic potential to derive the strain energy density of an elastic body, and then use the three-dimensional (3D) elasticity theory to analyze initial-boundary-value problems.

Yakobson *et al.*[2] postulated that the axial and the bending deformations of a SWCNT can be modeled by regarding the tube as a shell, used values of the bending and the axial stiffness derived by Robertson *et al.*[3] through MD simulations of SWCNTs with the Brenner potential, and found the shell wall thickness equal to 0.066 nm. They used this value of the wall thickness and of the corresponding Young's modulus to successfully correlate the buckling of a SWCNT due to axial loads to that of a shell. Sears and Batra[4] adopted a similar approach in that they equated the response of a SWCNT in axial and torsional deformations to that of a hollow cylinder composed of a linear elastic isotropic material and derived values of Young's modulus, the shear modulus, and the wall thickness. In the works of Robertson *et al.*[3] and Sears and Batra,[4] Poisson's ratio was found from changes in diameter induced during axial deformations of a tube. Sears and Batra[4] and Wang and Zhang[5] summarized the values of the wall thickness obtained by different authors using various approaches. Subsequently, Sears and Batra[6] correlated the buckling deformations of a SWCNT to those derived by using a shell theory, and also studied buckling of double- and triple-walled CNTs (DWCNTs and TWCNTs).

In view of the enormous literature on CNTs we briefly review only works on their vibrations. Suffice it to say that almost all works on SWCNTs have either assumed a value for the wall thickness, or have derived it by equating an experimental observation to that deduced from a structural mechanics model.

Sohlberg *et al.*[7] employed the solution of the wave equation, and the Euler–Bernoulli beam theory (EBBT) to relate vibrations of a SWCNT to those of its equivalent continuum structure (ECS). However, while studying the radial breathing mode (RBM) vibrations of a nanotube and of its ECS,

a)Electronic mail: rbatra@vt.edu.

 

they seem to have ignored the fact that radial deformations of a tube wall induce strains in both the axial and the circumferential directions. Yao and Lordi[8] studied the transverse vibrations of cantilever armchair SWCNTs due to thermal excitation. They conducted simulations at different temperatures, and found that the amplitude of vibration is directly proportional to the temperature, but the tube's natural frequencies are temperature independent. Using the EBBT and the wall thickness of 3.4 Å (the interlayer separation in bulk graphite), they found that Young's modulus $E$ decreases with an increase in the tube radius, and $E$ converges to 0.98 TPa. Except for the (5, 5) SWCNT, other SWCNTs in their simulations had aspect ratio $<7.5$ for which the EBBT may not give good results. Krishnan *et al.*[9] experimentally studied, in a transmission electron microscope (TEM), the thermally induced stochastic vibrations of cantilevered SWCNTs 23.4–36.8 nm in length and 1.0–1.5 nm in diameter. They modeled SWCNTs as Euler–Bernoulli beams with annular cross sections of wall thickness $h$ equal to 3.4 Å and found the average value of $E$ to be 1.25 TPa. Poncharal *et al.*[10] also used a TEM to study the vibrations of MWCNTs induced by an alternating voltage, employed the EBBT with tubes's ECSs to be solid circular cylinders of diameters 10 and 30 nm, and found $E$ to equal 1.2 and 0.2 TPa, respectively. They attributed the drop in the value of $E$ for the larger diameter tube to the onset of wavelike distortions in the tube.

Li and Chou[11] used a structural mechanics approach to study the vibrations of clamped-clamped SWCNTs and MWCNTs, represented the van der Waals interactions in a DWCNT by the Lennard-Jones potential, modeled covalent bonds between carbon atoms by truss elements, and computed frequencies of the fundamental and the higher modes of vibration of SWCNTs and DWCNTs. However, while discussing the results, they did not elaborate on limitations of the EBBT for computing the natural frequencies. Agrawal *et al.*[12] used MD simulations to calculate $E$ from frequencies of the longitudinal vibrations of cantilevered SWCNTs, and used the EBBT for studying the transverse vibrations. For tubes of aspect ratio $<25$, they found that the value of $E$ derived from the EBBT was 25% less than that obtained from frequencies of axial vibrations, and that the value of $E$ decreased with an increase in the radius of the armchair and the zigzag tubes. Taking $h=3.4$ Å they found that the average value of $E$ equaled 0.73 TPa and 0.82 TPa for the armchair and the zigzag tubes, respectively. Yoon *et al.*[13] studied the vibrations of DWCNTs with the Timoshenko beam theory (TBT), modeled them as double beams, and considered the effects of rotary inertia and shear deformations. Wang and Varadan[14] studied the one-dimensional wave propagation in CNTs and used the EBBT and the TBT to explain their results. Mir *et al.*[15] modeled zigzag and armchair SWCNTs by regarding bonds between carbon atoms as beams, and studied the effects of scaling in the geometry on modes of vibration of cantilevered SWCNTs.

Batra and Gupta[16] used MM simulations with the MM3 potential to compute the frequencies of axial, torsional, bending, and RBMs of tubes of the three helicities, aspect ratio (length/diameter) ~15, and radii ranging from 2 to 10 Å. They equated the frequencies of a SWCNT to those of a hollow cylinder of mean diameter equal to that of the tube and comprised of a linear elastic, homogeneous, and isotropic material. The frequencies of the cylinder were derived by using the 3D linear elasticity theory (LET) and the finite element method (FEM). They found average values of $E$ and $h$ to equal 3.3 TPa and 1 Å, respectively. These values imply that the axial stiffness $Eh$ of a SWCNT equals 54.08 eV/atom, which is 7% less than the 58.2 eV/atom determined by Robertson *et al.*[3] with the local density functional theory.

Here we explore the mechanics and the physics of free vibrations of relaxed zigzag SWCNTs with traction-free ends by conducting MM simulations with the MM3 potential that incorporates bond stretching, the change in angle between adjacent bonds, twisting of bonds, van der Waals forces, and the coupling among stretching, bending, and twisting deformations. The energy due to bond stretching has terms that are quadratic, cubic, and quartic in changes in the bond length, and is thus *not an even function* of the change in the bond length.

As for any other prismatic structure, the fundamental natural frequency of a SWCNT increases as its length decreases. However, for a fixed radius of a SWCNT, the mode of vibration of the lowest natural frequency may also be significantly affected by its length. For a SWCNT used as a nanomechanical resonator one needs to know not only the lowest natural frequency but also the corresponding mode shape for proper tuning.

Our simulations reveal that the vibrational response of zigzag SWCNTs cannot be simulated by modeling it as either a linear elastic shell or a 3D linear elastic isotropic hollow cylinder since the frequencies of the inextensional modes found through MM simulations saturate for large circumferential wave numbers, but those of the shell and the hollow cylinder do not. This is explained in terms of the molecular structure of a zigzag SWCNT.

## II. MM SIMULATIONS

The MM3 (Ref. 17) class II pairwise potential with both higher-order expansions and cross terms and type 2 (alkene) carbon atoms is appropriate for modeling CNTs due to the similarity between graphitic bonds in the nanotube and the aromatic protein structures for which the potential was constructed. The MM3 potential is given by Eq. (1) in which $U_s$, $U_\theta$, and $U_\phi$ are energies due to bond stretching, bending, and torsion, respectively; $U_{\mathrm{vdW}}$ is the potential of nonbonded van der Waals forces, and $U_{s\theta}$, $U_{\phi s}$, and $U_{\theta\theta'}$ represent the energies of cross interactions between stretch-bend, torsion-stretch, and bend-bend types of deformations, respectively. The parameters $r$, $\theta$, $\theta'$, and $\phi$ used in Eq. (1) are shown in Fig. 1. A subscript $e$ on a variable signifies its value in the configuration of the minimum potential energy. The total potential energy of a body equals the sum of the potential energies of all atoms in the body [indices $i$ and $j$ in Eq. (1) range over bonded atoms, and the index $k$ over all atoms].

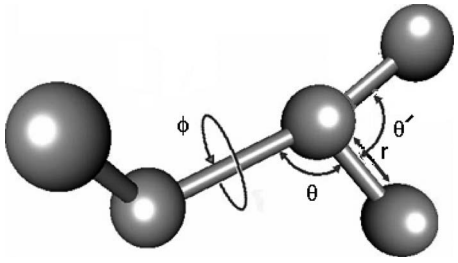


FIG. 1. Depictions of variables $r$, $\theta$, $\theta'$, and $\phi$ used in the expression for the MM3 potential.

$$U = \sum_i \sum_j (U_s + U_\theta + U_\phi + U_{s\theta} + U_{\phi s} + U_{\theta\theta'}) + \sum_i \sum_k U_{\mathrm{vdW}},$$

$$U_s = 71.94K_s(r - r_e)^2\left[1 - 2.55(r - r_e) + \left(\tfrac{7}{12}\right)2.55(r - r_e)^2\right],$$

$$U_\theta = 0.021\ 914K_\theta(\theta - \theta_e)^2[1 - 0.014(\theta - \theta_e) + 5.6 \times 10^{-5}(\theta - \theta_e)^2 - 7.0 \times 10^{-7}(\theta - \theta_e)^3 + 9.0 \times 10^{-10}(\theta - \theta_e)^4],$$

$$U_\phi = (V_1/2)(1 + \cos\phi) + (V_2/2)(1 - \cos 2\phi) + (V_3/2)(1 + \cos 3\phi),$$

$$U_{s\theta} = 2.511\ 18K_{s\theta}[(r - r_e) + (r' - r'_e)](\theta - \theta_e),$$

$$U_{\phi s} = 11.995(K_{\phi s}/2)(r - r_e)(1 + \cos 3\phi),$$

$$U_{\theta\theta'} = -0.021\ 914K_{\theta\theta'}(\theta - \theta_e)(\theta' - \theta'_e),$$

and

$$U_{\mathrm{vdW}} = \varepsilon_e\{-2.25(r_v/r)^6 + 1.84 \times 10^5 \exp[-12.0(r/r_v)]\}. \quad (1)$$

The values of constants $K_s$, $K_\theta$, $V_1$, $V_2$, $V_3$, $\varepsilon_e$, $r_v$, $K_{s\theta}$, $K_{\phi s}$, and $K_{\theta\theta'}$ taken from Ref. 17 are listed in Table I. Note that the van der Waals force between two atoms varies as $(r_v/r)^6$ and $\exp(-12r/r_v)$. The first term is the same as that in the Lennard-Jones potential, but the second term is different.

TABLE I. Values of parameters in the MM3 potential.

| Parameter | Value of the parameter |
|---|---|
| $K_s$ | 4.49 mdyn/Å |
| $K_\theta$ | 0.67 mdyn Å/rad$^2$ |
| $V_1$ | 0.185 kcal/mol |
| $V_2$ | 0.170 kcal/mol |
| $V_3$ | 0.520 kcal/mol |
| $\varepsilon_e$ | 0.027 kcal/mol |
| $r'_v$ | 2.04 Å |
| $K_{s\theta}$ | 0.130 mdyn/rad |
| $K_{\phi s}$ | 0.059 mdyn/rad |
| $K_{\theta\theta'}$ | 0.24 mdyn Å/rad$^2$ |

The motivation for assuming expressions for $U_s$, $U_\theta$, $U_\phi$, $U_{s\theta}$, $U_{\phi s}$, and $U_{\theta\theta'}$ is given in Ref. 17 and is omitted here.

As listed in Table 3 of Ref. 18 the MM3 (Ref. 17) potential used herein gives frequencies of RBMs, which agree well with their experimental values. Since no structural theory is used in this comparison, the close agreement between the computed and the experimental values provides one measure of the validity of the MM3 (Ref. 17) potential to model SWCNTs. Also, except for the Coulomb force due to point charges, expressions in the MM3 (Ref. 17) potential are essentially the same as those in the condensed-phase optimized molecular potentials for atomistic simulation studies often used to simulate deformations of polymeric materials.[19] Another indication of the suitability of the MM3 potential for SWCNTs is that the computed basal plane stiffness of 330 N/m (54.08 eV/atom) is very close to the experimental mean value of 340 N/m found by Lee *et al.*,[20] and is 7% less than the 58.2 eV/atom determined by Robertson *et al.*[3] with the local density functional theory.

A SWCNT is first relaxed to find the minimum energy configuration to within 0.001 kcal/(mol Å) rms without using any cut-off distance. Both ends of the tube are taken to be free and there is no ambiguity in simulating these boundary conditions in a laboratory. The module, VIBRATE, in computer code TINKER,[21] is used to calculate frequencies and mode shapes of vibration by computing eigenvalues and eigenvectors of the mass weighted Hessian. The first six eigenvalues of the Hessian equal zeros and are discarded since they correspond to three translational and three rotational rigid body modes. The eigenvector associated with an eigenvalue is used to identify the corresponding mode of vibration of a SWCNT. Furthermore, we find one-to-one correspondence between modes of vibration of a SWCNT computed through MM simulations, and those of a linear elastic and isotropic shell,[22] and of a linear elastic and isotropic 3D hollow cylinder; the latter are computed by using the FEM.

In the unrelaxed configuration, the diameter of an $(m,n)$ SWCNT is taken to equal the commonly used value $a_0[3(m^2+n^2+mn)]^{1/2}/\pi$ in the mechanics community. Here $a_0$ equals the distance between adjoining atoms. In the relaxed configuration, the diameter of a SWCNT equals the diameter of the circle passing through atoms on a plane perpendicular to the axis of the tube. Thus the effects of charge densities are ignored in the computation of the diameter of a SWCNT. For all SWCNTs studied herein, $a_0 = 1.42$ Å, and the bond length in the relaxed configuration equals 1.346 Å.

For a free-free SWCNT, a shell, and a hollow cylinder some modes of vibration do not involve a change in the axial length; the modes of vibration in which deformations do not vary axially are called the Rayleigh modes, and those in which deformations vary linearly in the axial direction are called the Love modes. The kinematics of inextensional deformations requires that the midsurface of the SWCNT and of either the shell or the hollow cylinder deform without stretching. For a circular hollow cylinder this necessitates that generators of the cylinder remain straight during vibration, as shown by the red line in Fig. 2(a). Both the Rayleigh and the Love modes of vibration generally correspond to the axial half wave number $j=0$, and are termed inextensional

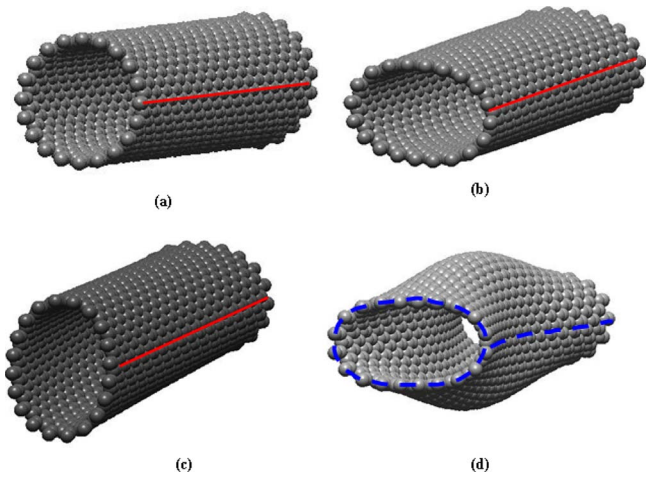


FIG. 2. (Color online) Modes of vibration of (20,0) SWCNT of aspect ratio 4.58: (a) tube in the relaxed state, (b) the lowest Rayleigh mode of frequency 18.95 $cm^{-1}$, (c) the lowest Love mode of frequency 19.12 $cm^{-1}$, and (d) the mode corresponding to $i=2$ and $j=1$ having frequency 22.34 $cm^{-1}$. A generating line of the cylindrical surface whose length remains unchanged during inextensional vibrations is shown in red color. In (d), two circumferential waves and a half axial wave are shown as dashed blue lines for a bending mode of vibration. Colored lines are visible only in the online version.

modes; Figs. 2(b) and 2(c) show the inextensional Rayleigh and Love modes for (20, 0) SWCNT of aspect ratio 4.58. The mode of vibration with the circumferential wave number $i=2$ and the axial half wave number $j=1$ is shown in Fig. 2(d).

## III. EXPRESSIONS FOR FREQUENCIES OF A SHELL

We summarize below the frequencies of different modes of vibration of a shell comprised of a linear elastic, homogeneous, and isotropic material. For inextensional deformations, the natural frequency $\omega_i^R$ of a Rayleigh mode of vibration is given by[22]

$$\omega_i^R = \frac{i(i^2-1)}{\sqrt{(i^2+1)}}\sqrt{\frac{h^2}{12r_e^2}}\left[\frac{1}{r_e}\sqrt{\frac{E}{\rho(1-\nu^2)}}\right], \quad i=2,3,4,\ldots, \tag{2}$$

where $h$, $r_e$, $E$, $\rho$, and $\nu$ are, respectively, the wall thickness, the mean radius, Young's modulus, the mass density, and Poisson's ratio. For a shell with aspect ratio of ~4.0 or greater, the frequency, $\omega_{\mathrm{RBM}}$, of the RBM is given by

$$\omega_{\mathrm{RBM}} = \frac{1}{r_e}\sqrt{\frac{E}{\rho(1-\nu^2)}}. \tag{3}$$

For aspect ratios <4.0, $\omega_{\mathrm{RBM}}$ given by Eq. (3) has an appreciable error.[22] Thus the wall thickness $h$ of the shell, corresponding to a SWCNT of aspect ratio ~4, in terms of $\omega_i^R$ and $\omega_{\mathrm{RBM}}$, is given by

$$h = \frac{\sqrt{12(i^2+1)}}{i(i^2-1)}\left(\frac{\omega_i^R}{\omega_{\mathrm{RBM}}}\right)r_e, \quad i=2,3,4,\ldots. \tag{4}$$

The frequency of a RBM of vibration is identified as a prominent $A_{1g}$ spectral line in the Raman spectroscope of a SWCNT.

The frequency $\omega_i^L$ of the Love mode of vibration of a shell of an *arbitrary aspect ratio* is given by[22]

$$\omega_i^L = \frac{i(i^2-1)}{\sqrt{(i^2+1)}}\sqrt{\frac{h^2}{12r_e^2}}\left[\frac{1}{r_e}\sqrt{\frac{E}{\rho(1-\nu^2)}}\right] \times \left[\frac{1+\dfrac{24(1-\nu)r_e^2}{i^2l_e^2}}{1+\dfrac{12r_e^2}{i^2(i^2+1)l_e^2}}\right]^{1/2}, \quad i=2,3,4,\ldots, \tag{5}$$

in which $l_e$ equals the length of the shell. Thus with an increase in the aspect ratio the frequency of the Love mode converges to that of the Rayleigh mode.

Frequencies $\omega_k^A$ of the axial modes of oscillations of a shell of aspect ratio >4, and $\omega_k^T$ of the torsional vibrations of a shell of any aspect ratio are given, respectively, by

$$\omega_k^A = \frac{k\pi}{l_e}\sqrt{\frac{E}{\rho}}, \quad k=1,2,3,\ldots, \tag{6}$$

$$\omega_k^T = \frac{k\pi}{l_e}\sqrt{\frac{G}{\rho}}, \quad k=1,2,3,\ldots, \tag{7}$$

where $G$ is the shear modulus of the shell material. For an isotropic linear elastic material, $E$, $G$, and $\nu$ are related by $E=2G(1+\nu)$. Thus Eqs. (6) and (7) give

$$\nu = \frac{1}{2}\left(\frac{\omega_k^A}{\omega_k^T}\right)^2 - 1, \quad k=1,2,3,\ldots.$$

### A. Effect of transverse inertia forces

For shells of aspect ratio <4, the transverse inertia effects are dominant and the frequencies of axial vibrations are given by[23]

$$\omega_k^A = \frac{k\pi}{\sqrt{\left(1+\dfrac{\nu^2\kappa^2k^2\pi^2}{l_e^2}\right)}}\left[\frac{1}{l_e}\sqrt{\frac{E}{\rho}}\right], \quad k=1,2,3,\ldots, \tag{8}$$

where $\kappa$ is the polar radius of gyration. That is, the consideration of transverse inertia decreases the fundamental frequencies of axial vibrations, and the determination of Poisson's ratio from frequencies requires *a priori* knowledge of the geometry of the shell. Furthermore, the frequency of the $k^{\mathrm{th}}$ mode does not equal $k$ times the frequency of the first mode of vibration. The elimination of $E$ from Eqs. (6) and (8) yields the following quadratic equation for $\nu$:

$$\nu^2\left(r_e^2+\frac{h^2}{4}\right)\left[\frac{k\pi\omega_k^A}{l_e\omega_k^T}\right]^2 - 2\nu + \left[\left(\frac{\omega_k^A}{\omega_k^T}\right)^2 - 2\right] = 0, \quad k=1,2,3,\ldots. \tag{9}$$

Similarly, the elimination of $E$ from Eqs. (5) and (7) yields the following expression for $h$:

TABLE II. Geometries of large aspect ratio SWCNTs, their frequencies from MM simulations, computed Poisson's ratio and wall thickness, and comparison with frequencies of the RBM found by other investigators.

| Tube $(n,m)$ | Radius $(r_e)$ (Å) | A. R. $(l_e/d_e)$ | $\omega^R$ $(i=2)$ $(cm^{-1})$ | $\omega^A$ $(k=1)$ $(cm^{-1})$ | $\omega^T$ $(k=1)$ $(cm^{-1})$ | $\omega_{RBM}$ $(cm^{-1})$ | $\nu$ | $h$ (Å) | Literature values of $\omega_{RBM}$ Lawler *et al.*[a] | Kurti *et al.*[b] | Kuzmany *et al.*[c] (Expt.) |
|---|---|---|---|---|---|---|---|---|---|---|---|
| (10, 0) | 3.713 | 15.200 | 53.323 | 29.633 | 18.732 | 290.463 | 0.251 | 0.879 | 294 | 298 | N. A. |
| (16, 0) | 5.937 | 15.263 | 27.781 | 18.329 | 11.633 | 181.747 | 0.241 | 1.172 | 177 | 188[d] | 185 |
| (20, 0) | 7.420 | 15.021 | 19.040 | 14.691 | 9.346 | 145.363 | 0.235 | 1.255 | N. A. | 150 | N. A. |

[a]Reference 24.
[b]Reference 25.
[c]Reference 26.
[d]Obtained from the expression for the RBM proposed by Kurti *et al.* (Ref. 25).

$$h^2 = \frac{6(i^2+1)(k\pi)^2 r_e^4(1-\nu)}{i^2(i^2-1)^2 l_e^2}\left(\frac{\omega_i^L}{\omega_k^T}\right)^2 \left[\frac{1+\frac{12r_e^2}{i^2(i^2+1)l_e^2}}{1+\frac{24(1-\nu)r_e^2}{i^2 l_e^2}}\right], \tag{10}$$

$$i = k+1, \quad k = 1,2,3,\ldots .$$

Thus from frequencies of the axial, the torsional, and the Love modes of vibration, one can first find $\nu$ from Eq. (9) and then $h$ from Eq. (10). The elimination of $h$ from Eqs. (9) and (10) yields a cubic equation for $\nu$, which has at least one real root that depends on the aspect ratio of the shell. However, $\omega_i^L/\omega_k^T$ depends on the mean radius $r_e$ of the shell.

## IV. COMPARISON OF PRESENTLY FOUND FREQUENCIES WITH THOSE IN LITERATURE

To validate our procedure and the applicability of the MM3 (Ref. 17) potential to SWCNTs we have listed in Table II frequencies, $\omega_{RBM}$ [in $cm^{-1}$=Hz/(speed of light in cm/s)], of RBMs ($A_{1g}$ symmetry mode) of three zigzag SWCNTs of aspect ratio ~15 found from our MM simulations, and those given in literature. It is evident that the presently computed values of $\omega_{RBM}$ are close to those reported in literature. We note that in these comparisons no ECS has been used. Thus the MM3 (Ref. 17) potential gives very good values of $\omega_{RBM}$. We have also listed frequencies of axial, torsional, and Rayleigh modes of vibration of the three SWCNTs.

The diameter of the (10, 0) SWCNT is 7.426 Å, which is greater than $3r_\nu$ ($r_\nu$=2.04 Å). Therefore, the van der Waals force between diametrically opposite atoms is negligible. Furthermore, in Table 3 of Ref. 16, the computed frequencies of the RBMs of the (10, 0) SWCNT from the MM simulations and the continuum mechanics approach were found to agree well with those found using *ab initio* methods by other authors. Thus the van der Waals force does not play a noticeable role for the (10, 0) SWCNT.

## V. COMPARISON OF NATURAL FREQUENCIES OF SWCNTs WITH THOSE OF A SHELL AND A HOLLOW CYLINDER

We now examine if the response of a zigzag SWCNT can be represented by that of either a shell or a hollow cylinder comprised of a linear elastic, homogeneous, and isotropic material. Accordingly, we compare frequencies of different modes of vibration of two arbitrarily chosen (20,0) and (36,0) zigzag SWCNTs of aspect ratios ~6 determined through MM simulations with those of a shell and a hollow cylinder found by using the commercial FE code ABAQUS.[27] The mean radii of the shell and the hollow cylinder are set equal to the radius of the SWCNT, and the wall thickness and values of material parameters of the shell and the cylinder are derived by equating frequencies of their axial, torsional, and the first inextensional modes of vibrations with the corresponding ones of the SWCNT found through the MM simulations. Table III lists the values of material and geometric parameters of a shell and a cylinder. It is clear that the computed wall thickness varies with the tube radius possibly due to the consideration of van der Waals forces between nonbonded atoms. There is no analog of this force in classical continuum mechanics. This force decays with the distance between two nonbonded atoms and its influence on mechanical deformations dies out for tubes of large radius as compared to that for tubes of small radius.

For brevity, we have listed in Table III results for only two SWCNTs; similar results computed by using the MM3 potential for 22 SWCNTs of different diameters and chiralities are given in Tables 2 and 3 of Ref. 16. These results

TABLE III. Frequencies of various vibrational modes and values of elastic moduli of SWCNTs for simulations with structural models. $n_c$ is the number of carbon atoms in MM simulations.

| SWCNT $(m,n)$ $n_c$ | Aspect ratio $(l_e/d_e)$ | Mode No. | Torsional mode $(cm^{-1})$ | Axial mode $(cm^{-1})$ | Love mode $(i=2)$ $(cm^{-1})$ | Rayleigh mode $(i=2)$ $(cm^{-1})$ | Thickness $(h)$ (Å) | Poisson's ratio $(\nu)$ | Young's modulus $(E)$ (TPa) |
|---|---|---|---|---|---|---|---|---|---|
| (20,0) | 5.671 | 1 | 24.856 | 39.112 | 19.085 | 19.011 | 1.25 | 0.24 | 2.7 |
| 1680 | | 2 | 49.689 | 77.612 | | | | | |
| (36,0) | 5.669 | 1 | 14.128 | 22.105 | 6.462 | 6.388 | 1.36 | 0.22 | 2.4 |
| 5436 | | 2 | 28.253 | 43.837 | | | | | |

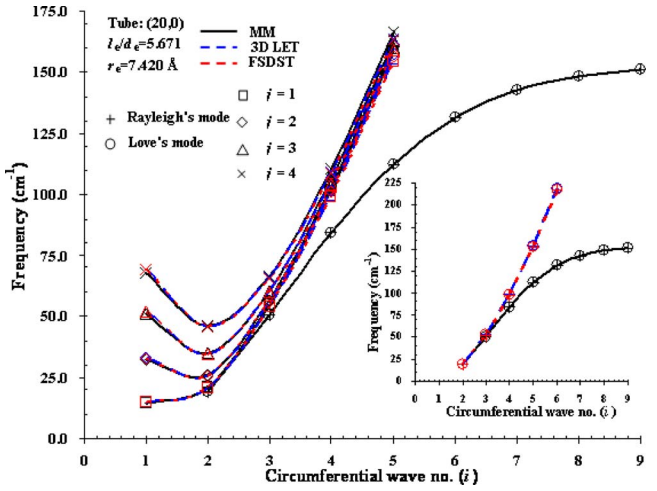


FIG. 3. (Color online) Variation with the circumferential wave number of the extensional and the inextensional mode frequencies of (20, 0) SWCNT found from MM simulations, of the shell obtained by using the FSDST and of the hollow cylinder. With an increase in the circumferential wave number, the inset shows saturation of the frequencies of inextensional modes found from the MM simulations but a monotonic rise in their values for the equivalent continuum structures.

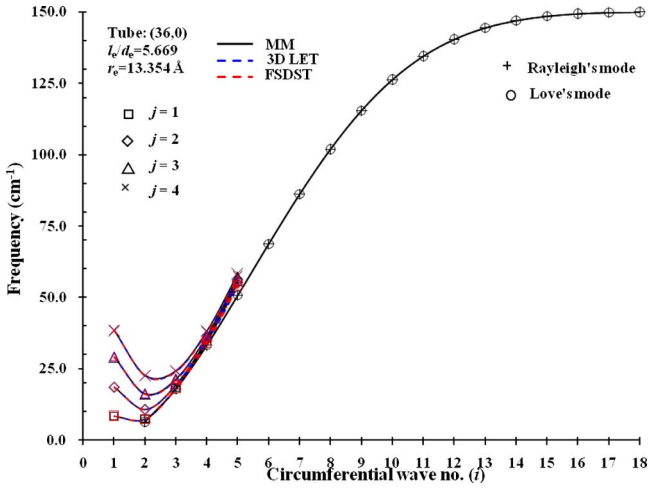


FIG. 4. (Color online) Variation with the circumferential wave number of the extensional and the inextensional mode frequencies of (36, 0) SWCNT found from MM simulations, of the shell obtained by using the FSDST and of the hollow cylinder.

show that the frequencies of the axial and the torsional modes of vibration obey Eqs. (6) and (7), as evidenced by the nearly constant value of $E$ found by using these equations. Thus the frequencies of the axial and the torsional modes of vibration are inversely proportional to the tube length. The $\omega_{\mathrm{RBM}}$ was found to be inversely proportional to the radius of the SWCNT in the unrelaxed configuration, and the constant of proportionality, 1135, found in Ref. 16 is close to the literature value of 1090–1170.

For the shell we use the first-order shear deformable shell theory[28] (FSDST) with the shear correction factor of 5/6. However, 3D deformations of the hollow cylinder are analyzed. For the FSDST, the FE mesh for the shell is comprised of 8-node shear deformable elements (S8R5), whereas the hollow cylinder is divided into 20-node brick elements (C3D20R). The FE meshes are refined successively until the computed frequencies converge to 0.01% of their values. The FE meshes for a hollow cylinder that gave converged frequencies for the (20, 0) and the (36, 0) SWCNTs had {39, 67} and {86, 149} elements (circumferential direction, axial direction); the corresponding FE meshes for the shell were {47, 84} and {86, 149}.

The frequencies of the extensional and the inextensional modes of vibration of (20, 0) SWCNT of aspect ratio 5.67 and of its equivalent shell and hollow cylinder are plotted in Fig. 3 with abscissa as the circumferential wave number. For *extensional modes* corresponding to the first few axial half wave numbers and the first few circumferential wave numbers, the MM simulation results overlap those from the FSDST and the 3D LET applied to the hollow cylinder. When the MM simulation results are taken as the reference, the absolute maximum errors in the results from the FSDST and the LET are ~2.8% and ~2.3%, respectively. However, for the *inextensional modes*, the frequency of oscillations increases with an increase in the circumferential wave number for the shell and the hollow cylinder, but that from the MM simulations seems to saturate near the circumferential wave number of 10; this difference is shown clearly in the inset of Fig. 3. A similar behavior, depicted in Fig. 4, is observed for the larger diameter (36, 0) SWCNT of aspect ratio 5.67. The frequencies of various extensional and inextensional modes of vibration and computed with different methods/theories are listed in Table IV. It can be seen that the absolute maximum difference in the results for the extensional modes from different approaches is ~2.4%. However, for inextensional modes of vibration, the results from the FSDST and the LET deviate from the MM simulation results by ~5.3%. The sudden jump in the difference in the frequencies of the SWCNT and of its ECSs in going from the circumferential wave number of 4–5 is due to the saturation of frequencies of the SWCNT but not those of its ECSs. This discrepancy between frequencies of the SWCNT and of its ECS increases with an increase in the circumferential wave number.

The results from the MM simulations for (16, 0) SWCNT of aspect ratios 6.07 and 2.32 are displayed in Figs. 5 and 6, for (21, 0) SWCNT of aspect ratio 3.58 in Fig. 7, and for (20, 0) SWCNT of aspect ratio 1.04 in Fig. 8. These evince that the saturation of frequencies of inextensional modes with an increase in the circumferential wave number is independent of the aspect ratio and the diameter of zigzag SWCNTs. Consistent with the expressions for frequencies reviewed in Sec. III, for the small aspect ratio (20, 0) the tube frequencies of the Rayleigh and the Love modes for low circumferential wave numbers are different.

We note that the EBBT and the TBT also do not predict the saturation of frequencies of inextensional modes of vibration. Of course, one does not expect the EBBT to predict well deformations of tubes of aspect ratio ~6 or less. The 3D LET is applicable to bodies of all shapes and sizes. The frequencies of inextensional modes of vibration of hollow cylinders equivalent in shape and size to the SWCNT computed using the 3D LET do not exhibit the saturation phenomenon seen in the results from the MM simulations of zigzag SWCNTs.

TABLE IV. Comparison of frequencies of extensional and inextensional modes of vibration of the (36, 0) SWCNT found from MM simulations with those of the shell using the FSDST, and of the hollow cylinder using the 3D LET and the FEM.

| Axial half wave number | SWCNT | | (36,0) | | | | |
|---|---|---|---|---|---|---|---|
| | Circumferential wave number | | 1 | 2 | 3 | 4 | 5 |
| 1 | \|%Error\| with respect to MM | MM ($cm^{-1}$) | 8.455 | 7.481 | 18.477 | 34.685 | 55.368 |
| | | 3D-LET | 0.021 | 1.382 | 1.199 | 1.728 | 2.330 |
| | | FSDST | 0.054 | 1.575 | 1.413 | 1.898 | 2.441 |
| 2 | \|%Error\| with respect to MM | MM ($cm^{-1}$) | 18.556 | 10.819 | 19.536 | 35.416 | 55.983 |
| | | 3D-LET | 0.044 | 1.003 | 0.995 | 1.361 | 1.958 |
| | | FSDST | 0.030 | 1.137 | 1.198 | 1.531 | 2.069 |
| 3 | \|%Error\| with respect to MM | MM ($cm^{-1}$) | 29.143 | 16.278 | 21.491 | 36.650 | 57.016 |
| | | 3D-LET | 0.146 | 0.731 | 0.947 | 1.150 | 1.691 |
| | | FSDST | 0.076 | 0.817 | 1.120 | 1.313 | 1.800 |
| 4 | \|%Error\| with respect to MM | MM ($cm^{-1}$) | 38.480 | 22.747 | 24.450 | 38.435 | 58.480 |
| | | 3D-LET | 0.236 | 0.553 | 0.974 | 1.033 | 1.503 |
| | | FSDST | 0.179 | 0.600 | 1.098 | 1.182 | 1.608 |
| Inextensional modes | | | | | | | |
| Rayleigh mode | \|%Error\| with respect to MM | MM ($cm^{-1}$) | ⋯ | 6.388 | 17.878 | 33.248 | 50.734 |
| | | 3D-LET | ⋯ | 1.626 | 1.309 | 0.731 | 5.418 |
| | | FSDST | ⋯ | 1.838 | 1.522 | 0.556 | 5.299 |
| Love mode | \|%Error\| with respect to MM | MM ($cm^{-1}$) | ⋯ | 6.462 | 17.903 | 33.249 | 50.734 |
| | | 3D-LET | ⋯ | 1.318 | 0.801 | 1.081 | 5.633 |
| | | FSDST | ⋯ | 1.532 | 1.016 | 0.905 | 5.514 |

## VI. EXPLANATION OF THE SATURATION OF FREQUENCIES

The saturation of frequencies with an increase in the circumferential wave number for a zigzag tube can be attributed to the arrangement of bonds on its cylindrical surface. For an armchair tube $\sigma$-bonds perpendicular to the tube's axis, depicted in Fig. 9, provide resistance to bending deformations. However, for a zigzag tube $\sigma$-bonds are parallel to the axis of the tube and may behave like mechanisms, which after some circumferential wave patterns do not offer any resistance to bending deformations. We *hypothesize* that for a $(n,\ 0)$ zigzag tube, the saturation occurs at the circumferential wave number of $(n-1)/2$ or $(n/2)$, where $n$ is odd or even. This is due to the impossibility of the formation of full wave patterns beyond $(n-1)/2$ or $(n/2)$. Accordingly, the frequencies of the inextensional modes for the (36, 0) and the

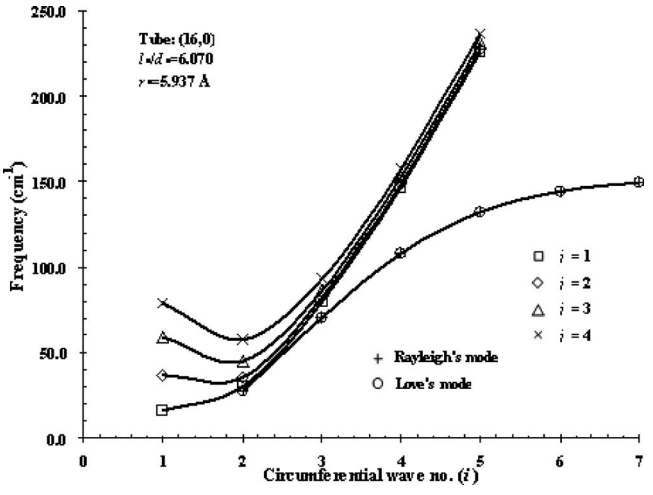


FIG. 5. For (16, 0) SWCNT, variation with the circumferential wave number of frequencies of various combinations of the axial and the circumferential wave numbers, and the Rayleigh and the Love inextensional modes found through MM simulations.

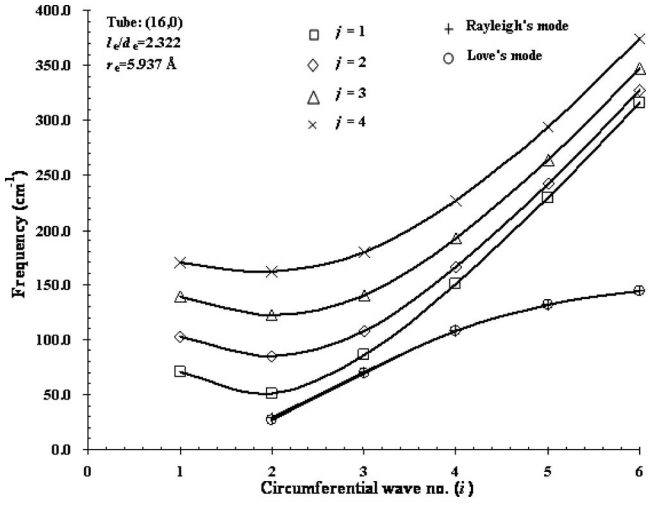


FIG. 6. For (16, 0) SWCNT, variation with the circumferential wave number of frequencies of various combinations of the axial and the circumferential wave numbers, and the Rayleigh and the Love inextensional modes found through MM simulations.

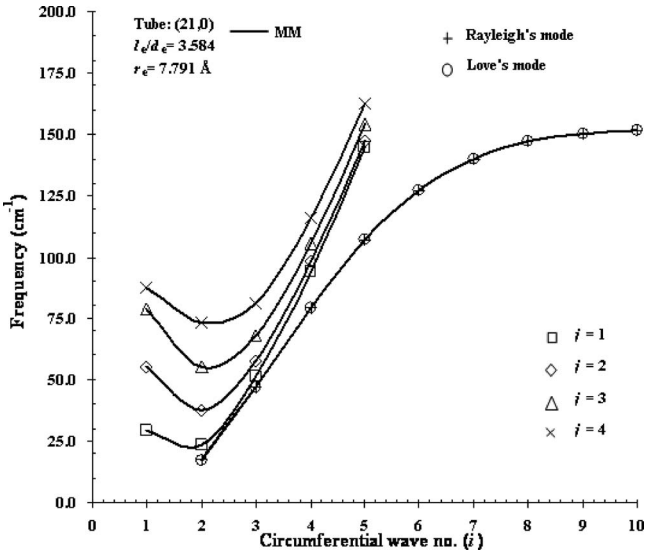


FIG. 7. For (21, 0) SWCNT, variation with the circumferential wave number of frequencies of various combinations of the axial and the circumferential wave numbers, and the Rayleigh and the Love inextensional modes found through MM simulations.

(21, 0) SWCNTs will saturate at circumferential wave numbers of 18 and 10, respectively, as confirmed by the results depicted in Figs. 3–8.

As far as we can determine, this saturation of frequencies of zigzag tubes has not been reported before.

## VII. DISCUSSION

We note that our MM simulations of vibrations of armchair and chiral SWCNTs with the MM3 potential and of the same aspect ratios as those considered here do not reveal the saturation of frequencies of inextensional modes of vibration. Furthermore, the frequencies of ECSs comprised of isotropic linear elastic materials match well with those of the corresponding SWCNTs. Thus only zigzag SWCNTs exhibit

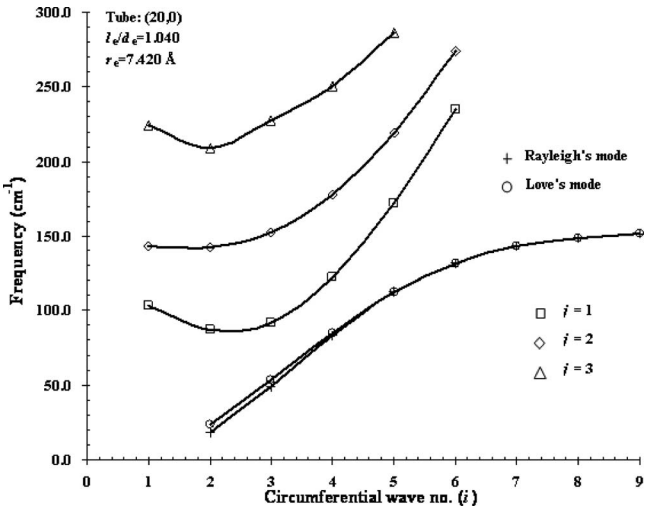


FIG. 8. For (20, 0) SWCNT, variation with the circumferential wave number of frequencies of various combinations of the axial and the circumferential wave numbers, and the Rayleigh and the Love inextensional modes found through MM simulations.

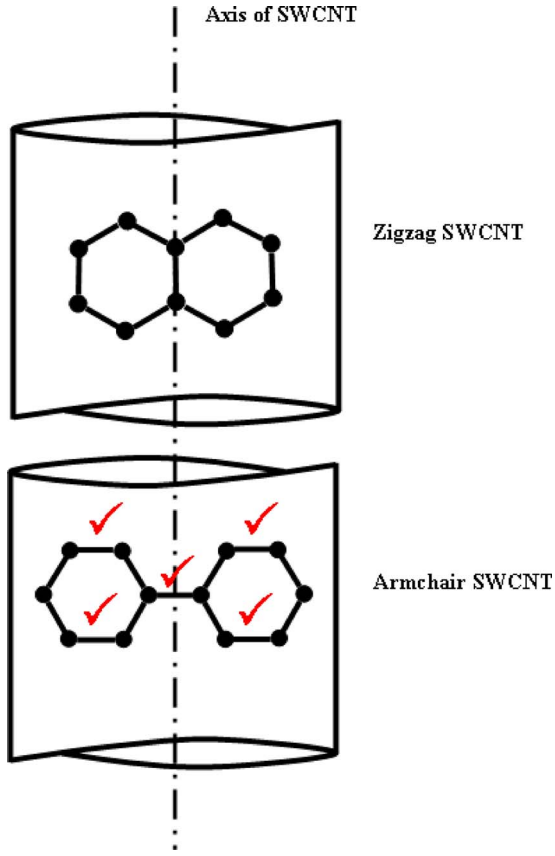


FIG. 9. (Color online) Schematics of bond arrangements in a zigzag and an armchair SWCNT. For the armchair tube, bonds that participate in bending during inextensional modes are shown by red check marks. The zigzag tubes do not have this bond arrangement that offers resistance to bending deformations during vibrations with circumferential wave numbers greater than 1.

the saturation of frequencies of inextensional modes due to their molecular structure as elaborated above.

In nearly all works on SWCNTs, including that of Batra's group, it has been tacitly assumed that the value of either a material constant or a geometric parameter derived by equating one quantity obtained either from experiments or from MM simulations to that from a structural theory is valid for all other deformations. The present work shows that this is not the case, and one should specify the range of validity of the continuum/structural model by studying different modes of deformation using MM simulations and the corresponding structural theories. For inextensional vibrations of zigzag tubes, even the 3D LET is *incapable* of predicting the saturation of frequencies. Thus *not* all deformations of a SWCNT can be studied from those of its ECS. The problem of finding all types of deformations for which the SWCNT and its ECS give different responses is a challenging exercise and is left for future work.

The present study also provides an example of a class of deformations for which the response of a zigzag SWCNT differs from that of chiral and armchair SWCNTs.

## VIII. CONCLUSIONS

We have studied vibrations of zigzag SWCNTs using MM simulations with the MM3 potential, and found parameters of a shell and a hollow cylinder whose frequencies of

the first inextensional mode, RBM, and axial and torsional modes of vibration are equal to the corresponding ones of the SWCNT. The frequencies of the shell are found by using the FSDST, and those of the cylinder with the 3D LET. The frequencies of the extensional modes of vibration of the shell and the cylinder essentially coincide with the corresponding ones of the SWCNT. However, with an increase in the circumferential wave number, the frequencies of the inextensional modes of vibration of the shell and the cylinder monotonically increase, but those of the corresponding SWCNT saturate to a steady value. This deviation in the frequencies implies that a shell and a hollow cylinder cannot be used to study the inextensional vibrations of a zigzag SWCNT. We have explained this saturation of frequencies of the tube in terms of its molecular structure.

This study provides an example of a class of deformations in which the responses of zigzag tubes differ from those of armchair and chiral SWCNTs, and also points to the need of providing limits of applicability of a structural model of a SWCNT.

## ACKNOWLEDGMENTS

This work was supported by the Office of Naval Research Grant No. N00014-06-1-0567 to Virginia Polytechnic Institute and State University with Dr. Y. D. S. Rajapakse as the program manager. Partial support was also provided by Virginia Tech's Institute for Critical Technologies and Applied Sciences. Views expressed in the paper are those of authors, and neither of the funding agencies nor of their institutions.

[1]S. Iijima, Nature (London) **354**, 56 (1991).
[2]B. I. Yakobson, C. J. Barbee, and J. Bernholc, Phys. Rev. Lett. **76**, 2511 (1996).
[3]D. H. Robertson, D. W. Brenner, and J. W. Mintmire, Phys. Rev. B **45**, 12592 (1992).
[4]A. Sears and R. C. Batra, Phys. Rev. B **69**, 235406 (2004).
[5]C. Y. Wang and L. C. Zhang, Nanotechnology **19**, 075705 (2008).
[6]A. Sears and R. C. Batra, Phys. Rev. B **73**, 085410 (2006).
[7]K. Sohlberg, B. G. Sumpter, R. E. Tuzun, and D. W. Noid, Nanotechnology **9**, 30 (1998).
[8]N. Yao and V. Lordi, J. Appl. Phys. **84**, 1939 (1998).
[9]A. Krishnan, E. Dujardin, T. W. Ebbesen, P. N. Yianilos, and M. M. J. Treacy, Phys. Rev. B **58**, 14013 (1998).
[10]P. Poncharal, Z. L. Wang, D. Urarte, and W. A. de Heer, Science **283**, 1513 (1999).
[11]C. Li and T. W. Chou, Appl. Phys. Lett. **84**, 121 (2004).
[12]P. M. Agrawal, B. S. Sudalayandi, L. M. Raff, and R. Komanduri, Comput. Mater. Sci. **38**, 271 (2006).
[13]J. Yoon, C. Q. Ru, and A. Mioduchowski, ASME J. Appl. Mech. **72**, 10 (2005).
[14]Q. Wang and V. K. Varadan, Int. J. Solids Struct. **43**, 254 (2006).
[15]M. Mir, A. Hosseini, and G. H. Majzoobi, Comput. Mater. Sci. **43**, 540 (2008).
[16]R. C. Batra and S. S. Gupta, ASME J. Appl. Mech. **75**, 061010 (2008).
[17]N. L. Allinger, Y. H. Yuh, and J.-H. Lii, J. Am. Chem. Soc. **111**, 8551 (1989).
[18]S. S. Gupta and R. C. Batra, Comput. Mater. Sci. **43**, 715 (2008).
[19]S. Yu, S. Yang, and M. Cho, Polymer **50**, 945 (2009).
[20]C. Lee, X. Wei, W. Kysar, and J. Hone, Science **321**, 385 (2008).
[21]J. W. Ponder, computer code TINKER molecular modelling package 4.2, 2004.
[22]R. D. Blevins, *Formulas for Natural Frequencies and Mode Shapes* (Van Nostrand Reinhold, New York, 1979).
[23]A. W. Leissa and J. So, J. Acoust. Soc. Am. **98**, 2122 (1995).
[24]H. M. Lawler, D. Areshkin, J. W. Mintmire, and C. T. White, Phys. Rev. B **72**, 233403 (2005).
[25]J. Kurti, G. Kresse, and H. Kuzmany, Phys. Rev. B **58**, R8869 (1998).
[26]H. Kuzmany, B. Burger, M. Hulman, J. Kurti, A. G. Rinzler, and R. E. Smalley, Europhys. Lett. **44**, 518 (1998).
[27]ABAQUS User's Manual, 2006, finite element computer code 6.7.
[28]S. Timoshenko and S. Woinowsky-Krieger, *Theory of Plates and Shells*, 2nd ed. (McGraw-Hill, New York, 1959).